Available online at www.sciencedirect.com
SCIENCE DIRECT
Biochemical and Biophysical Research Communications 339 (2006) 115–121
BBRC
www.elsevier.com/locate/ybbrc

# Structural and biochemical characterization of DSL ribozyme ☆

Souta Horie [a], Yoshiya Ikawa [b], Tan Inoue [a,*]

[a] Graduate School of Biostudies, Kyoto University, Kyoto 606-8502, Japan
[b] Department of Chemistry and Biochemistry, Graduate School of Engineering, Kyushu University, 819-0395 Fukuoka, Japan

Received 25 October 2005
Available online 9 November 2005

**Abstract**

We recently reported on the molecular design and synthesis of a new RNA ligase ribozyme (DSL), whose active site was selected from a sequence library consisting of 30 random nucleotides set on a defined 3D structure of a designed RNA scaffold. In this study, we report on the structural and biochemical analyses of DSL. Structural analysis indicates that the active site, which consists of the selected sequence, attaches to the folded scaffold as designed. To see whether DSL resembles known ribozymes, a biochemical assay was performed. Metal-dependent kinetic studies suggest that the ligase requires $Mg^{2+}$ ions. The replacement of $Mg^{2+}$ with $Co(NH_3)_6^{3+}$ prohibits the reaction, indicating that DSL requires innersphere coordination of $Mg^{2+}$ for a ligation reaction. The results show that DSL has requirements similar to those of previously reported catalytic RNAs.


*Keywords:* Ribozyme; Kinetic analysis; Structural analysis; RNA ligase; Mechanism

A molecular modeling technique based on the RNA structural biology enables the design and construction of artificial RNAs with defined 3D structures [1–3]. In one example, we reported on the design and construction of a self-folding RNA consisting of three helices assembled in a defined 3D structure by forming two sets of tertiary interactions [3]. An RNA ligase ribozyme termed DSL was constructed by installing a catalytic unit on the self-folding RNA [4]. In vitro selection was performed to isolate the catalytic unit from a library consisting of 30 random nucleotides inserted at a site near the reaction site in the model 3D structure. To further investigate DSL, we performed structural and biochemical characterization using DSL-1S [4], its most active derivative (Fig. 1).

## Materials and methods

*RNA preparation.* Ribozymes were transcribed from PCR-amplified templates by T7 RNA polymerase either in the absence or presence of [α-$^{32}$P]GTP. Transcripts were purified by 5% denaturing PAGE. For a 5′-labeled ribozyme preparation, ribozymes were treated with calf intestinal alkaline phosphatase, then phosphorylated using T4 polynucleotide kinase in the presence of [γ-$^{32}$P]ATP and purified by 5% denaturing PAGE. For the construction of DSL-1S mutants, DNA template coding DSL-1S was amplified by PCR in the presence of appropriate primers. For DMS modification and $Pb^{2+}$ cleavage, 25 additional nucleotides, 5′-CAGU CUCAUUGCCCACUUAGGCAGA-3′, were added to the 3′-end of DSL-1S to monitor the modification or cleavage profile of the 3′-end region of DSL-1S. Substrate RNA was also added to the 5′-end of DSL-1S so that the ribozyme was actively conformed. The substrate RNA 5′-CGU ACACGUACUCACGCGUAUACAGUCCAC-3′ was purchased from Dharmacon (Colorado, USA).

*DMS modification and reverse transcription.* Forty picomoles of RNA was incubated in water (29 μl) at 95 °C for 1 min and then cooled. Twenty microliters of 2.5× reaction buffer (500 mM KCl, 75 mM Tris, and 125 mM $MgCl_2$, pH 7.5) was added to this solution and the mixture was equilibrated at 37 °C for 10 min. Then, 1 μl of 10% DMS in ethanol was added and incubated at 37 °C for 5 min. Reactions were stopped with 3 μl of 1 M 2-mercaptoethanol. The samples were centrifuged to precipitate the RNAs after adding 5 μl of 3 M sodium acetate, 1 μl glycogen, and 125 μl ethanol. To detect the DMS-modified adenines and cytidines, one-fifth of

☆ *Abbreviations*: DSL, designed and selected ligase; Tris, tris(hydroxymethyl)aminomethane; DMS, dimethyl sulfate.

* Corresponding author. Fax: +81 75 753 3996.
*E-mail address:* tan@kuchem.kyoto-u.ac.jp (T. Inoue).

0006-291X/$ - see front matter © 2005 Elsevier Inc. All rights reserved.
doi:10.1016/j.bbrc.2005.11.007

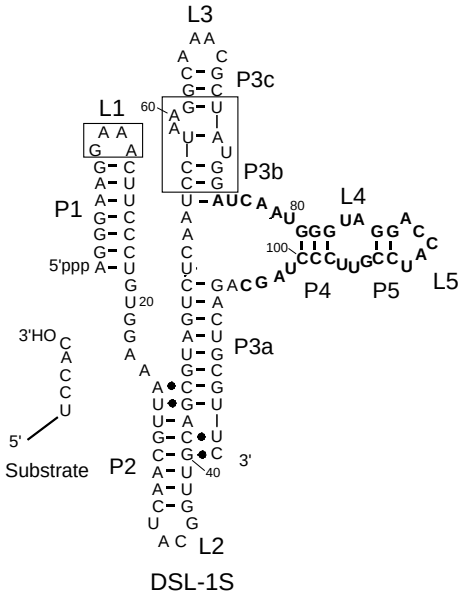


Fig. 1. Secondary structure of DSL-1S. Sequence selected from 30 random nucleotides is in boldface. GAAA loop and 11 nt receptor are boxed.

the modified RNAs (8.0 mol) were subjected to reverse transcription with AMV reverse transcriptase XL (Takara Shuzo, Japan) with [5′-$^{32}$P]-labeled DNA primer complementary to 26 nucleotides at the 3′ end of the respective RNA. Products were electrophoresed on 6% denaturing PAGE and quantitated with a Bio Imaging Analyzer. The extent of modification was classified based on the signal intensity of the band determined with Quantity One gel-imaging software (Bio-Rad): weakly modified and strongly modified bands correspond to the quantified intensity between 224 and 230 int, and higher than 230 int, respectively.

*$Pb^{2+}$ cleavage.* One picomole of 5′-labeled DSL-1S was incubated at 95 °C in water (5 μl) for 1 min and then cooled. To this solution was added 4 μl of 2.5× reaction buffer (500 mM KCl, 75 mM Tris, and 125 mM $MgCl_2$, pH 7.5), and the mixture was equilibrated at 37 °C for 10 min. One microliter of 1 mM $Pb(OAc)_2$ was added and then incubated for 30 min at 37 °C. The reactions were stopped with 2 μl of 0.5 M EDTA. The samples were centrifuged to precipitate the RNAs after adding 5 μl of 3 M sodium acetate, 1 μl glycogen, and 125 μl ethanol. Cleavage fragments were separated by 6% PAGE and quantitated with a Bio Imaging Analyzer.

*General kinetic assays.* Ribozymes were heated at 80 °C in water (15 μl) for 5 min and then cooled to 37 °C over 5 min. Twelve microliters of 2.5× reaction buffer (500 mM KCl, 75 mM Tris, and 125 mM $MgCl_2$) was added to this solution, and the mixture was equilibrated at 37 °C for 5 min. Reactions were initiated by adding 3 μl of 10 μM substrate RNA to the ribozyme solution. The final reaction conditions were 50 nM ribozyme, 1 μM substrate, 50 mM $MgCl_2$, 200 mM KCl, and 30 mM Tris (pH 7.5). Aliquots of 5 μl were taken at various time points and quenched with 2 volume of a stop solution (80% formamide, 87.5 mM EDTA). The resulting products were resolved with 5% PAGE and quantitated with a Bio Imaging Analyzer BAS 2500 (Fuji Film, Japan). Rate constants were derived from at least two independent experiments. Each rate was determined by fitting the data to the following equation:

$$\text{Fraction reacted} = F_a(1 - e^{-kt}),$$

where $t$ equals time, $k$ equals the catalysis rate, and $F_a$ equals the fraction of substrate · ribozyme in an active conformation [5]. DeltaGraph 4.0 (Polaroid) was used to fit the data to a single exponential.

*pH-dependent kinetics.* The buffers were Bis-Tris (pH 6.5–7.0) and Tris (pH 7.5–9.0). As mentioned in the general kinetic protocols, RNA solutions were prepared with corresponding buffers, as were the remaining procedures.

*Temperature-dependent kinetics.* The pH of the buffer was adjusted to pH 7.5 at each temperature because the pH of Tris buffers fluctuates approximately 0.028 pH units per 1 °C.

*Metal ion-dependent kinetics and $Co(NH_3)_6^{3+}$ inhibition.* Metal ion-dependent experiments were performed in a manner similar to the general kinetic assays, except that 50 mM $MgCl_2$ was replaced with 50 mM divalent metal ion ($CaCl_2$, $BaCl_2$, $MnCl_2$, $CoCl_2$, $NiCl_2$, $CuCl_2$, or $ZnCl_2$). Cobalt (III) hexamine was dissolved in water containing 1 mM EDTA to prepare a 125 mM stock solution. The inhibition assay was performed in a manner similar to the general kinetic assays, except that a reaction buffer containing various concentrations of $Co(NH_3)_6^{3+}$ was used.

## Results and discussion

### *Overall structure*

To determine whether DSL folds into the designed structure, we previously constructed derivatives that were predicted to have defective tertiary interactions. Mutation at the base-triples moderately lowered activity while the loop–receptor interaction significantly lowered it [4]. In this study, we attempted to confirm whether the parental self-folding RNA retained its original 3D-structure after installation of the catalytic unit.

The secondary structure of DSL-1S was investigated using dimethyl sulfate (DMS) that specifically methylates the free N1 of adenine and the free N3 of cytidine (Figs. 2A and B). In the 11 nt receptor, A59 and A71 were protected from modification under our standard conditions (50 mM $Mg^{2+}$): the N1 of A59 and the N1 of A71 participating in $Mg^{2+}$-dependent tertiary interactions cannot be modified [6,7]. The data are consistent with the previous result which indicated the presence of a tertiary interaction between the GAAA tetraloop and the 11 nt receptor. However, the secondary structure of P1 region was not determined because of smeared bands presumably due to pausing of reverse transcription at some unusual local structure in the P1 region (Fig. 2A). A47, which Zuker algorithm predicts to base pair with, U109 was weakly modified, suggesting that the A–U pair is breathing under the conditions we employed [8].

To further confirm the result, we constructed an almost inactive DSL-1S (mut-GUGA) mutant containing a GUGA loop in place of the original GAAA loop [4] (Fig. 2C). A59 and A71 of mut-GUGA were equally modified in the presence or absence of $Mg^{2+}$, indicating that the 11 nt receptor specifically interacts with the GAAA loop in DSL-1S. The data strongly support the designed model structure (Fig. 1).

No significant alteration of the structure of the scaffold was observed after installing the catalytic unit. When combined with the results of the preceding paper [4], this indicates that our synthetic strategy—"Addition of a catalytic unit on a designed RNA scaffold"—is both valid and practical.

### *Characterization of catalytic core*

In the catalytic unit (positions 75–104), the DMS modification was consistent with the secondary structure

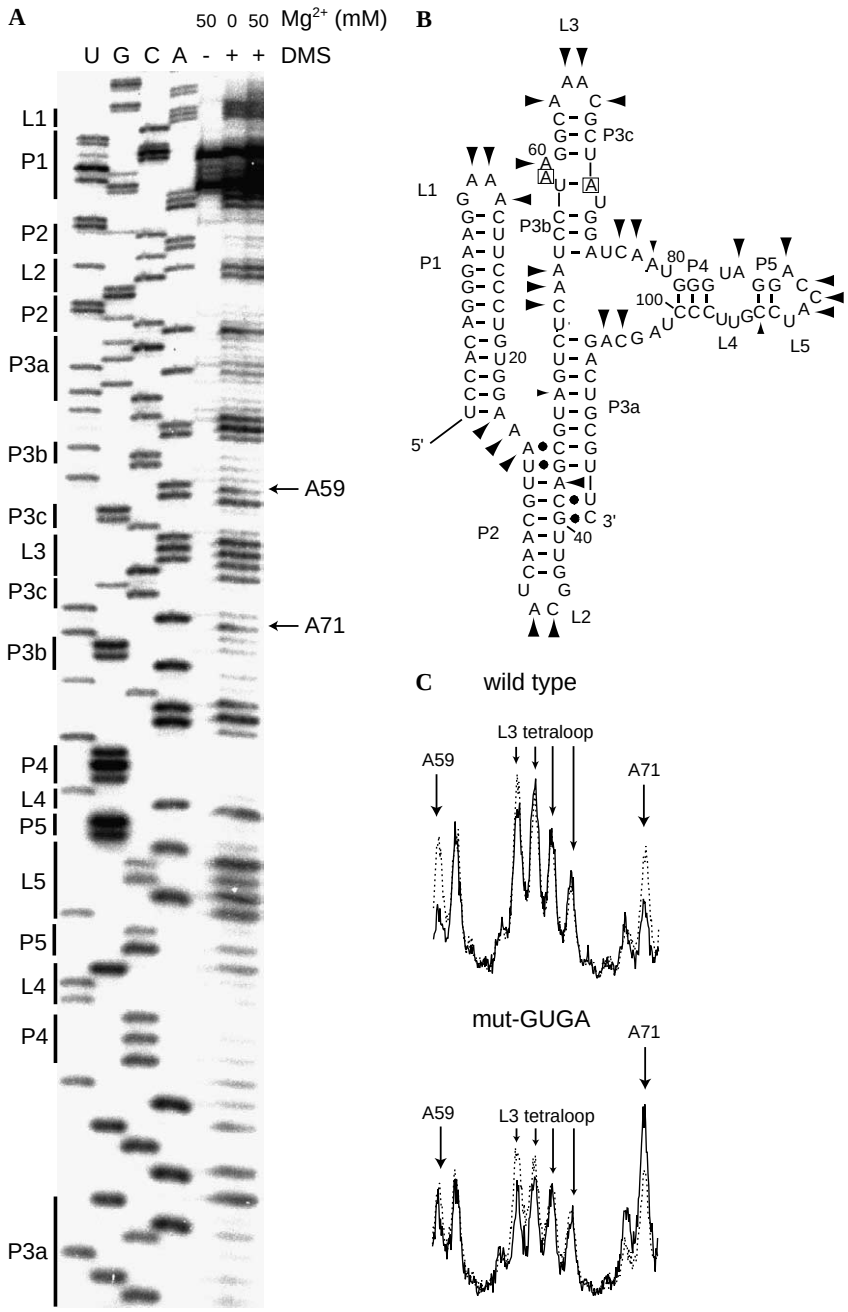


Fig. 2. (A) DMS modification of DSL-1S. A59 and A71 are protected from modification in the presence of 50 mM $Mg^{2+}$ (Arrow). (B) Summary of DMS modification in the presence of 50 mM $Mg^{2+}$. Large and small arrowheads denote strong and weak modification, respectively. A59 and A71 are boxed. (C) Intensity of the modification of wild type DSL-1S (top) or mut-GUGA mutant (bottom) in the absence (dotted lines) or presence (solid lines) of 50 mM $Mg^{2+}$.

predicted with the Zuker algorithm the except for position A54 and A102. A54 was predicted to form a base pair with U76 [4]. The base pair is located at the end of the stem and verges on the three-way junction consisting of P3a, P3b, and P4, indicating that it is less stable than the standard A–U base pair within the helix. A102 was modified very weakly as shown on the gel, suggesting that the local structure around the site prevents the modification or that N1 of A102 participates in the hydrogen bonding network in the catalytic core. Alternatively, it seems also possible that A102 is paired with U80 to form an alternative structure at and around P4. Weak modification was detected at C94 presumably due to the low melting temperature of the stem structure.

To identify the essential residue(s) in the selected sequence, 15 new mutants were prepared and investigated (Fig. 3, Table 1). We previously reported that 17 nucleotides in the catalytic unit (Fig. 3, boldface type) are invariable [4]. ΔL4/5, a mutant in which U84–U97 were substituted with six nucleotides (5′-CUUCGG-3′) comprising

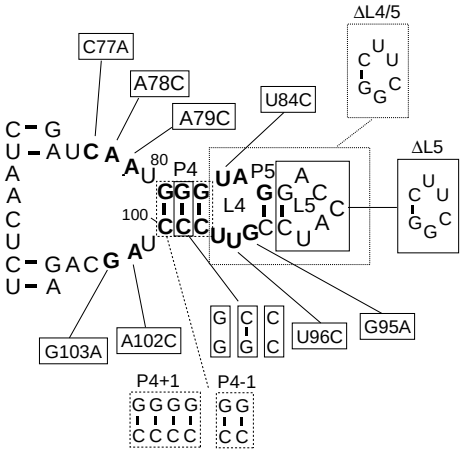


Fig. 3. Mutational studies on DSL-1S in catalytic unit. Seventeen invariable positions are in boldface [4].

Table 1
Relative rates of reaction of DSL-1S mutants

| Mutation | Rate relative to DSL-1S |
|---|---|
| C77A | Activity not detected[a] |
| A78C | Activity not detected[a] |
| A79C | 0.03 |
| A102C | Activity not detected[a] |
| G103A | 0.05 |
| U84C | 0.03 |
| G95A | 0.48 |
| U96C | 0.21 |
| G82C | Activity not detected[a] |
| C99G | 0.04 |
| G82C, C99G | 0.02 |
| ΔL4/5 | Activity not detected[a] |
| ΔL5 | 1.1 |
| P4 + 1 | Activity not detected[a] |
| P4 − 1 | Activity not detected[a] |

Relative rate of each mutant was determined by comparison of its $k_{obs}$ with wild type $k_{obs} = 3.3 \times 10^{-2}$ min$^{-1}$, in 30 mM Tris, pH 7.5, 50 mM $Mg^{2+}$, and 200 mM KCl.

[a] Fraction of ribozyme reacted was less than 0.003 after 1 h incubation.

a stable tetraloop, exhibited no catalytic activity. In contrast, the sequence of a terminal pentaloop (L5) is highly diversified [4], suggesting that the loop is nonessential for the catalysis. Consistent with this observation, a DSL-1S mutant (ΔL5 mutant) having a stable UUCG loop in place of the original L5 pentaloop was as active as DSL-1S.

Single base mutation at the three-way junction (C77A, A78C, A79C, A102C or G103A) or on the 5′ side of L4 (U84C) resulted in very weak or no activity. However, single mutation at the 3′ side of L4, G95A, or U96C, retained 48% or 21% of the activity compared with DSL-1S, respectively. The results indicate that G95 and U96 are not as critical as other invariable bases in the mechanism of catalysis even though they behaved as invariable ones during the second selection [4]. Perhaps, G95 and U96 can fine-tune the conformation of the catalytic site, when compared with A95 and C96, respectively. As anticipated from the previous study, G82C or C99G, both of which disrupt the invariable G–C base pair in P4, resulted in an inactive ribozyme [4]. Interestingly, the compensatory mutations were unable to recover the activity (Fig. 3, Table 1). Moreover, two additional mutants containing an extended or shortened P4 helix (P4 + 1 or P4 − 1) were inactive. These results indicate that a particular combination of base pairings in P4 (81GGG83: 98CCC100 pairs) is important for constituting an active site. Perhaps, the P4 stem functions as part of the catalytic site or it determines neighboring conformation(s) to form a catalytic site.

(Note: to minimize disruption of the parental secondary structure of the unit, the secondary structure of each mutant was examined using the Zuker algorithm [8]. We used neither the A85 nor the U97 mutant because none of the base-substitutions at these positions were predicted to maintain the parental secondary structure.)

### *Metal ion binding*

The cleavage of RNA with $Pb^{2+}$ is often used to identify $Mg^{2+}$ binding sites in RNA because $Pb^{2+}$ can occupy $Mg^{2+}$ binding sites [9–11]. The protection of $Pb^{2+}$ cleavage in the presence of $Mg^{2+}$is indicative of the binding site for $Mg^{2+}$[9–11]. To identify $Mg^{2+}$ binding sites, DSL-1S was incubated with 100 μM $Pb^{2+}$ in the presence or absence of $Mg^{2+}$ (Fig. 4). At A53, A59, A78–U80, and U101–G103, the cleavages were prominent or indistinctive in the presence or absence of 10 mM $Mg^{2+}$, respectively. These sites are located in the three-way junction except A59 in the 11 nt receptor. Thus, it appears that A53, A78–U80, and U101–G103 constitute the $Mg^{2+}$ binding site(s) used in the folding mechanism and/or catalysis both independently and in tandem. The mutations at the lead cleavage sites (Fig. 4) drastically reduced activity whereas those separated from the cleavage sites (G95A, U96C) caused a moderate reduction (Fig. 3, Table 1), suggesting that the $Mg^{2+}$ binding pockets are highly structured at the active site. If this were the case, a minor structural alteration at that site should cause considerable loss of activity.

The ribozyme's catalytic activity was investigated by employing divalent metal ions other the than $Mg^{2+}$ ion (Fig. 5). Like most natural ribozymes that are highly active when $Mn^{2+}$ is substituted for $Mg^{2+}$, the observed rate constant ($k_{obs}$) 0.20 min$^{-1}$ at 50 mM $Mn^{2+}$ was approximately 6-fold higher than that of 0.033 min$^{-1}$ at 50 mM $Mg^{2+}$ in the presence of 1 μM substrate RNA. To further investigate the effect of $Mg^{2+}$ or $Mn^{2+}$, $k_{obs}$ was determined as a function of their $Mg^{2+}$ and $Mn^{2+}$ concentrations (Fig. 6). The profiles showed a sigmoidal-like curve rather than a Michaelis–Menten curve, suggesting that two or more metal ions bind to the ribozyme. This is consistent with the lead-cleavage data indicate the presence of two distinct $Mg^{2+}$ binding sites at the 11 nt receptor and the three-way junction. Like most natural ribozymes [12–15], DSL-1S was inactive with $Ba^{2+}$, $Ni^{2+}$, $Cu^{2+}$, and $Zn^{2+}$ (Fig. 5). $Co^{2+}$ weakly supported the catalysis, presumably

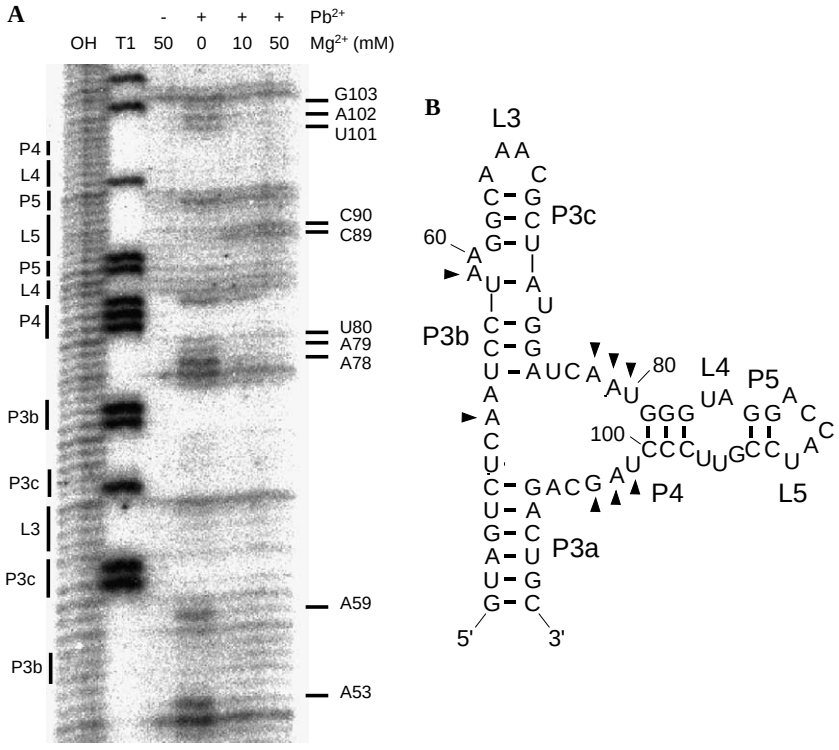


Fig. 4. (A) Lead cleavage of DSL-1S. OH and T1 denote alkaline hydrolysis and T1 endonuclease ladders, respectively. (B) Summary of the cleavage reaction. Arrowheads denote cleavage sites which exhibited prominent or indistinctive signal in the absence or presence of 10 mM of $Mg^{2+}$, respectively.

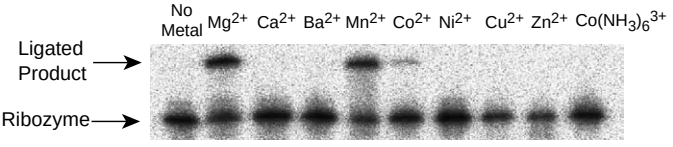


Fig. 5. Divalent metal ion dependence of ligation. Reactions were carried out for 20 min in presence of 50 mM divalent metal ion, in 200 mM KCl, and 30 mM Tris, pH 7.5.

because: (i) its ionic radius (0.75 Å) is similar to that of $Mg^{2+}$ (0.72 Å) or $Mn^{2+}$ (0.69 Å) and (ii) it prefers to bind to a phosphate like $Mg^{2+}$ [16].

$Co(NH_3)_6^{3+}$ can replace hydrated $Mg^{2+}$ coordinated with RNA because it has a similar size and geometry to that of $Mg(H_2O)_6^{2+}$ [9–11,17–21]. Several ribozymes are active when $Mg^{2+}$ is substituted with $Co(NH_3)_6^{3+}$ [18,19,21]. Theoretically, $Co(NH_3)_6^{3+}$ conducts the catalysis performed by $Mg^{2+}$ via an outersphere interaction, however, it inhibits the catalysis if the reaction requires $Mg^{2+}$ via an innersphere interaction [9–11,18–21]. To investigate the coordination of $Mg^{2+}$ in DSL-1S, we attempted a reaction with $Co(NH_3)_6^{3+}$ in the absence of $Mg^{2+}$. Ligation activity was lost, suggesting that DSL-1S requires innersphere metal ion coordination for catalysis (Fig. 5).

To further investigate the effects of $Co(NH_3)_6^{3+}$, the ligation rate was determined by titrating $Co(NH_3)_6^{3+}$ ions in the presence of 50 mM $Mg^{2+}$. As shown in Fig. 7, approximately 10 mM $Co(NH_3)_6^{3+}$ reduced the activity

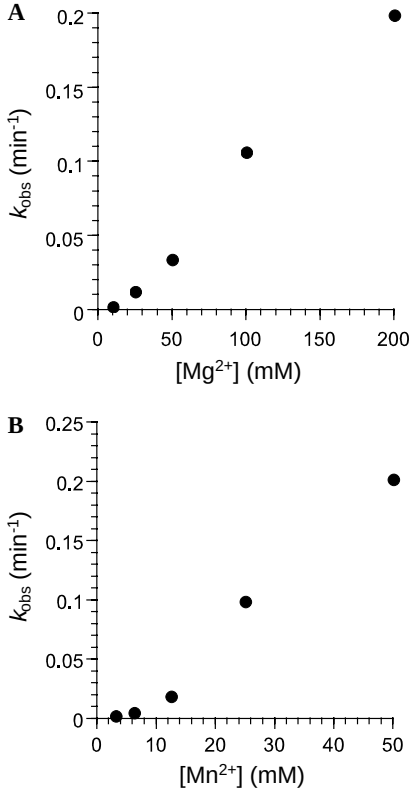


Fig. 6. Catalytic activity of DSL-1S vs $Mg^{2+}$ (A) or $Mn^{2+}$ (B) concentration. Reaction conditions are described in Materials and methods.

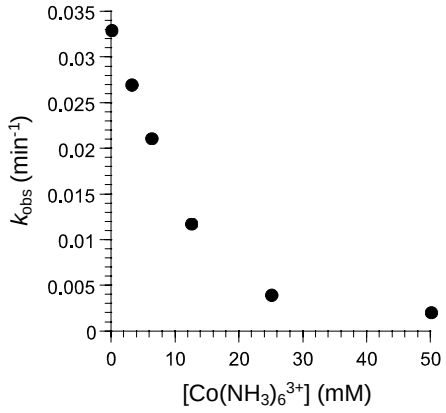


Fig. 7. $Co(NH_3)_6^{3+}$ inhibition assay. Depression of DSL-1S activity in the presence of 50 mM $Mg^{2+}$, as increasing concentrations of $Co(NH_3)_6^{3+}$ are added.

to a half-maximal. This suggests that $Co(NH_3)_6^{3+}$ can replace a $Mg^{2+}$ ion but cannot act as metal ion cofactor for catalysis or that its binding to certain site(s) induces an inactive conformation of the ribozyme. Similar observations were reported for the ribozymes that require inner-sphere $Mg^{2+}$ interaction [10,11].

*Kinetic analysis*

The maximum reaction rate ($k_{cat}$) and the Michaelis constant ($K_M$) were determined under our standard conditions (50 mM $MgCl_2$, 200 mM KCl, and 30 mM Tris, pH 7.5). The observed rate was plotted as a function of the concentration of the substrate (data not shown). The values for $k_{cat}$ and $K_M$ were 0.066 $min^{-1}$ and 940 nM, respectively ($k_{cat}/K_M = 7.0 \times 10^4$ $M^{-1}$ $min^{-1}$). Thus, the activity of DSL-1S is comparable to those of ligase ribozymes previously reported by Robertson and Ellington [22] (0.012 $min^{-1}$) and Jeager et al. [23] (0.26 $min^{-1}$).

The pH dependence of the ligation rate was investigated. The plot (pH vs log $k_{obs}$, Fig. 8) was linear between pH 6.5 and 8.5. The slope of the best-fit line to the data points between pH 6.5 and pH 8.5 was 1.4. Direct correspondence between the hydroxide ion concentration and the reaction rate was often observed for other ribozymes but interpretation is highly complicated [12,18,24–30].

Activation energy for ligation was determined to be 29.0 kcal/mol by the Arrhenius plot, which was linear in the range of 5–37 °C (Fig. 9). This linearity suggests the presence of a single rate-limiting step because the plot should be nonlinear if two or more steps participate in the rate determination as observed in the hammerhead ribozyme [31,32]. The deviation from linearity observed at 45 °C suggests that the substrate–ribozyme complex or the tertiary structure of the ribozyme starts to melt at this temperature. As described above, P5 perhaps melts under 45 °C, suggesting that its role is insignificant in holding the tertiary structure of the catalytic core. This is consistent with the fact that C94 at P5 is conserved incompletely [4]. The activation energy was converted to thermodynamic activation parameters using the Eyring equation. The calculated $\Delta H^{\ddagger}$ and $\Delta S^{\ddagger}$ values at 37 °C were 28.4 kcal/mol and 21.1 e.u., respectively. Note that the release of water molecules from hydrated $Mg^{2+}$ has been proposed as a cause of the positive $\Delta S^{\ddagger}$ value observed in the phosphoester transfer reaction by the *Tetrahymena* group I intron ribozyme, although the event responsible for the DSL positive $\Delta S^{\ddagger}$ value is currently unknown [33].

In this paper, we reported on the fundamental parameters relevant to the ligation activity of the DSL-1S ribozyme. In conclusion, the structural analyses confirmed that (i) DSL-1S retains the designed structure and that (ii) the residues required for the catalysis are present in the designed catalytic core. It was also found that the requirements for catalysis by DSL-1S differ little from those of previously known ribozymes. The results confirm that our strategy, which is based on molecular design at a 3D level, is valid for the design and synthesis of a ribozyme.

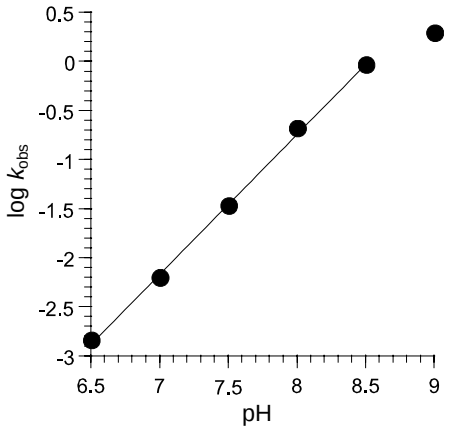


Fig. 8. pH dependence of ligation. Reaction conditions are described in Materials and methods.

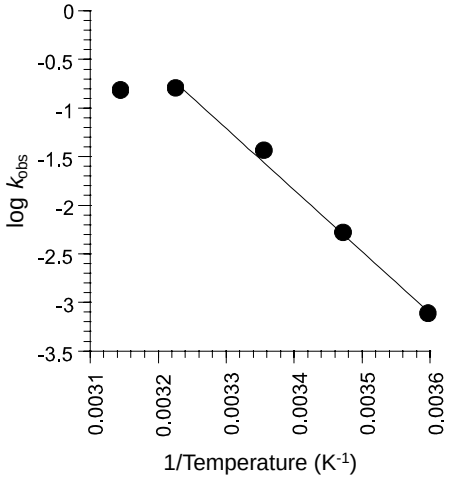


Fig. 9. Arrhenius plot for temperature dependence of ligation.

## Acknowledgments

This work was supported by Grants-in-Aid for Scientific Research in Priority Areas (Inoue and Ikawa) from the Ministry of Education, Science, Sports and Culture, Japan, and the Inamori, Iketani, and Kyushu University Foundations (Ikawa).

## References

[1] L. Jaeger, E. Westhof, N.B. Leontis, TectoRNA: modular assembly units for the construction of RNA nano-objects, Nucleic Acids Res. 29 (2001) 455–463.
[2] L. Jaeger, N.B. Leontis, Tecto-RNA: one-dimensional self-assembly through tertiary interactions, Angew. Chem. Int. Ed. 39 (2000) 2521–2524.
[3] Y. Ikawa, K. Fukada, S. Watanabe, H. Shiraishi, T. Inoue, Design, construction, and analysis of a novel class of self-folding RNA, Structure 10 (2002) 527–534.
[4] Y. Ikawa, K. Tsuda, S. Matsumura, T. Inoue, De novo synthesis and development of an RNA enzyme, Proc. Natl. Acad. Sci. USA 101 (2004) 13750–13755.
[5] N.H. Bergman, W.K. Johnston, D.P. Bartel, Kinetic framework for ligation by an efficient RNA ligase ribozyme, Biochemistry 39 (2000) 3115–3123.
[6] J.H. Cate, A.R. Gooding, E. Podell, K. Zhou, B.L. Golden, C.E. Kundrot, T.R. Cech, J.A. Doudna, Crystal structure of a group I ribozyme domain: principles of RNA packing, Science 273 (1996) 1678–1685.
[7] J.H. Cate, A.R. Gooding, E. Podell, K. Zhou, B.L. Golden, A.A. Szewczak, C.E. Kundrot, T.R. Cech, J.A. Doudna, RNA tertiary structure mediation by adenosine platforms, Science 273 (1996) 1696–1699.
[8] M. Zuker, Mfold web server for nucleic acid folding and hybridization prediction, Nucleic Acids Res. 31 (2003) 3406–3415.
[9] A. Flynn-Charlebois, N. Lee, H. Suga, A single metal ion plays structural and chemical roles in an aminoacyl-transferase ribozyme, Biochemistry 40 (2001) 13623–13632.
[10] A. Vaidya, H. Suga, Diverse roles of metal ions in acyl-transferase ribozymes, Biochemistry 40 (2001) 7200–7210.
[11] N. Lee, H. Suga, Essential roles of innersphere metal ions for the formation of the glutamine binding site in a bifunctional ribozyme, Biochemistry 40 (2001) 13633–13643.
[12] D. Smith, N.R. Pace, Multiple magnesium ions in the ribonuclease P reaction mechanism, Biochemistry 32 (1993) 5273–5281.
[13] S.C. Dahm, O.C. Uhlenbeck, Role of divalent metal ions in the hammerhead RNA cleavage reaction, Biochemistry 30 (1991) 9464–9469.
[14] H.N. Wu, Y.J. Lin, F.P. Lin, S. Makino, M.F. Chang, M.M. Lai, Human hepatitis delta virus RNA subfragments contain an autocleavage activity, Proc. Natl. Acad. Sci. USA 86 (1989) 1831–1835.
[15] C.A. Grosshans, T.R. Cech, Metal ion requirements for sequence-specific endoribonuclease activity of the Tetrahymena ribozyme, Biochemistry 28 (1989) 6888–6894.
[16] G.L. Eichhorn, Y.A. Shin, Interaction of metal ions with polynucleotides and related compounds. XII. The relative effect of various metal ions on DNA helicity, J. Am. Chem. Soc. 90 (1968) 7323–7328.
[17] A.L. Feig, O.C. Uhlenbeck, The role of metal ions in RNA biochemistry, in: R.F. Gesteland, T.R. Cech, J.F. Atkins (Eds.), The RNA World Second Edition, Cold Spring Harbor Laboratory press, Cold Spring Harbor, NY, 1999, pp. 287–319.
[18] H. Suga, J.A. Cowan, J.W. Szostak, Unusual metal ion catalysis in an acyl-transferase ribozyme, Biochemistry 37 (1998) 10118–10125.
[19] K.J. Young, F. Gill, J.A. Grasby, Metal ions play a passive role in the hairpin ribozyme catalysed reaction, Nucleic Acids Res. 25 (1997) 3760–3766.
[20] R. Jou, J.A. Cowan, Ribonuclease H activation by inert transition-metal complexes. Mechanistic probes for metallocofactors: insights on the metallobiochemistry of divalent magnesium ion, J. Am. Chem. Soc. 113 (1991) 6685–6686.
[21] E.A. Curtis, D.P. Bartel, The hammerhead cleavage reaction in monovalent cations, RNA 7 (2001) 546–552.
[22] M.P. Robertson, A.D. Ellington, In vitro selection of an allosteric ribozyme that transduces analytes to amplicons, Nat. Biotechnol. 17 (1999) 62–66.
[23] L. Jaeger, M.C. Wright, G.F. Joyce, A complex ligase ribozyme evolved in vitro from a group I ribozyme domain, Proc. Natl. Acad. Sci. USA 96 (1999) 14712–14717.
[24] D. Herschlag, M. Khosla, Comparison of pH dependencies of the Tetrahymena ribozyme reactions with RNA 2′-substituted and phosphorothioate substrates reveals a rate-limiting conformational step, Biochemistry 33 (1994) 5291–5297.
[25] A.M. Pyle, J.B. Green, Building a kinetic framework for group II intron ribozyme activity: quantitation of interdomain binding and reaction rate, Biochemistry 33 (1994) 2716–2725.
[26] T. Pan, B. Dichtl, O.C. Uhlenbeck, Properties of an in vitro selected $Pb^{2+}$ cleavage motif, Biochemistry 33 (1994) 9561–9565.
[27] L.F. Landweber, I.D. Pokrovskaya, Emergence of a dual-catalytic RNA with metal-specific cleavage and ligase activities: the spandrels of RNA evolution, Proc. Natl. Acad. Sci. USA 96 (1999) 173–178.
[28] S. Nakano, D.M. Chadalavada, P.C. Bevilacqua, General acid–base catalysis in the mechanism of a hepatitis delta virus ribozyme, Science 287 (2000) 1493–1497.
[29] D. Lazarev, I. Puskarz, R.R. Breaker, Substrate specificity and reaction kinetics of an X-motif ribozyme, RNA 9 (2003) 688–697.
[30] S.C. Dahm, W.B. Derrick, O.C. Uhlenbeck, Evidence for the role of solvated metal hydroxide in the hammerhead cleavage mechanism, Biochemistry 32 (1993) 13040–13045.
[31] Y. Takagi, K. Taira, Temperature-dependent change in the rate-determining step in a reaction catalyzed by a hammerhead ribozyme, FEBS Lett. 361 (1995) 273–276.
[32] A. Peracchi, Origins of the temperature dependence of hammerhead ribozyme catalysis, Nucleic Acids Res. 27 (1999) 2875–2882.
[33] T.S. McConnell, T.R. Cech, A positive entropy change for guanosine binding and for the chemical step in the Tetrahymena ribozyme reaction, Biochemistry 34 (1995) 4056–4140.